ELSEVIER

Catalysis Today 66 (2001) 225–232

CATALYSIS TODAY

www.elsevier.com/locate/cattod

Influence of column hardware on the performance of reactive distillation columns

R. Baur [a], R. Taylor [b], R. Krishna [a,*]

[a] Department of Chemical Engineering, University of Amsterdam, Nieuwe Achtergracht 166, 1018 WV Amsterdam, The Netherlands
[b] Department of chemical Engineering, Clarkson University, Potsdam, NY 13676, USA

Abstract

We compare the performance of an MTBE synthesis column using two different hardware configurations: (1) a sieve tray column in which the catalyst particles, encased inside wire gauze envelopes, placed along the liquid flow path; (2) a column filled with catalytically active packing of Raschig ring shape. The columns simulations are performed using a rigorous nonequilibrium model. Using the bottoms flow rate of MTBE as continuation parameter it is shown that the two different hardware configurations exhibit significantly different bifurcation diagrams. The sensitivity of this bifurcation diagram has been studied with varying (a) methanol feed, (b) iso-butene feed, (c) inert feed and (d) reflux ratio. We show that the cross-flow contacting on the sieve tray configuration is beneficial to conversion. © 2001 Elsevier Science B.V. All rights reserved.

Keywords: Reactive distillation; Equilibrium stage model; Nonequilibrium stage model; Multiple steady states; Maxwell–Stefan equations; Methyl *tert*-butyl ether synthesis; Packed column; Sieve tray column

1. Introduction

There is currently a great deal of academic and industrial interest in reactive (catalytic) distillation [1]. Both homogeneous and heterogeneous catalysed chemical reactions can be carried out in a reactive distillation (RD) column. There are three possible benefits of RD operation: (1) higher conversions are obtained for equilibrium-limited reactions due to shifting of the equilibrium to the right; (2) improved selectivity is obtained because of removal of products from the reaction zone and preventing these from undergoing further reaction to by-products; (3) benefits of heat integration are obtained because the heat generated in the chemical reactions is used for vaporisation. Hot spot formation is therefore prevented.

For heterogeneously catalysed RD processes packed columns (random packed or structured) or tray columns could be used [1–6]. In this paper we compare the influence of column hardware choice on the performance of an RD column for MTBE synthesis. The major objective is to demonstrate the importance of hardware selection on column performance. We use the nonequilibrium (NEQ) model for simulation purposes; this model takes proper account of interphase heat and mass transfer.

2. NEQ model development and simulation details

A schematic representation of the NEQ model is shown in Fig. 1. This NEQ stage may represent a tray or section of packing. The development of the material balances, component balances, interphase transport equations and reaction rate equations are the same as developed in our earlier papers [7–14]. Our model

---

[*] Corresponding author. Tel.: +31-20-525-7007;
fax: +31-20-525-5604.
E-mail address: krishna@its.chem.uva.nl (R. Krishna).

0920-5861/01/$ – see front matter © 2001 Elsevier Science B.V. All rights reserved.
PII: S0920-5861(00)00653-2

Nomenclature

a	interfacial area (m^2)
c	number of components (dimensionless)
$\text{Đ}_{i,k}$	Maxwell–Stefan diffusivity (m^2 s^{-1})
E	energy transfer rate (J s^{-1})
f	component feed stream (mol s^{-1})
F^{V}, F^{L}	vapour and liquid feedstream (mol s^{-1})
h	heat transfer coefficient (W m^{-2} K^{-1})
H	molar enthalpy (J mol^{-1})
K	vapour–liquid equilibrium constant (–)
L	liquid flow rate (mol s^{-1})
N	Mass transfer rate (mol s^{-1})
p_j	stage pressure (Pa)
Q	heat duty (J s^{-1})
Q_{L}	liquid flow rate across tray (m^3/s)
r	number of reactions (dimensionless)
R	gas constant (J mol^{-1} K^{-1})
$R_{\mathrm{m,j}}$	reaction rate (mol m^{-3} s^{-1})
T	temperature (K)
W	weir length (m)
x	mole fraction in the liquid phase (dimensionless)
y	mole fraction in the vapour phase (dimensionless)

Greek symbols

ε	reaction volume (m^3)
η	dimensionless coordinate (dimensionless)
κ	mass transfer coefficient (m s^{-1})
μ	chemical potential (J mol^{-1})
ν	stoichiometric coefficient (dimensionless)

formulation can deal with any number of reactions and the component molar balances for the vapour and liquid phases are

$$V_j y_{i,j} - V_{j+1} y_{i,j+1} - f_{i,j}^{\mathrm{V}} + N_{i,j}^{\mathrm{V}} = 0 \tag{1}$$

$$L_j x_{i,j} - L_{j-1} x_{i,j-1} - f_{i,j}^{\mathrm{L}} - N_{i,j}^{\mathrm{L}} - \sum_{m=1}^{r} \nu_{i,m} R_{m,j} \varepsilon = 0 \tag{2}$$

where $N_{i,j}$ is the interfacial mass transfer rate and $R_{m,j}$ the rate of reaction m on stage j. $\nu_{i,m}$ represents the stoichiometric coefficient of component i in reaction m and ε_j the reaction volume. For homogeneous reactions this is given by the total liquid holdup on stage j. For heterogeneous reactions, employing the pseudo-homogeneous description, this is given by the total amount of catalyst present on the stage under consideration. The overall molar balances are obtained by summing Eqs. (1) and (2) over the total number (c) of components in the mixture. The $N_{i,j}$ are related to the chemical potential gradients in either phase by the generalised Maxwell–Stefan equations [15–17]

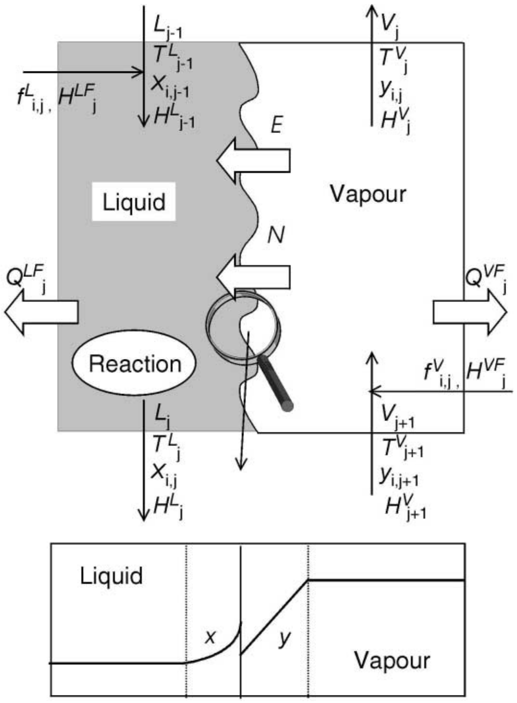

Fig. 1. NEQ model.

$$\frac{x_{i,j}}{RT_j} \frac{\partial \mu_{i,j}^{\mathrm{L}}}{\partial \eta} = \sum_{k=1}^{c} \frac{x_{i,j} N_{k,j}^{\mathrm{L}} - x_{k,j} N_{i,j}^{\mathrm{L}}}{c_{t,j}^{\mathrm{L}} (\kappa_{i,k}^{\mathrm{L}} a)_j} \tag{3}$$

with a similar relation for the vapour phase. The $\kappa_{i,k}^{\mathrm{L}}$ represents the mass transfer coefficient of the i–k pair in the liquid phase; this coefficient is estimated from information on the corresponding Maxwell–Stefan diffusivity $\text{Đ}_{i,k}$ using the standard procedures discussed in Taylor and Krishna [15]. Only $c - 1$ of Eqs. (3) are independent. The mole fraction of the cth component is obtained by the summation equations for both phases. The enthalpy balances for both vapour and liquid phase are

$$V_j H_j^{\mathrm{V}} - V_{j+1} H_{j+1}^{\mathrm{V}} - F_j^{\mathrm{V}} H_j^{\mathrm{VF}} + E_j^{\mathrm{V}} + Q_j^{\mathrm{V}} \tag{4}$$

$$L_j H_j^{\mathrm{L}} - L_{j-1} H_{j-1}^{\mathrm{L}} - F_j^{\mathrm{L}} H_j^{\mathrm{LF}} - E_j^{\mathrm{L}} + Q_j^{\mathrm{L}} \tag{5}$$

where the interphase energy transfer rates E_j (equal in both phases) have conductive and convective contributions

$$E_j^{\mathrm{L}} = -h_j^{\mathrm{L}} a \frac{\partial T^{\mathrm{L}}}{\partial \eta} + \sum_{i=1}^{c} N_{i,j}^{\mathrm{L}} H_{i,j}^{\mathrm{L}} \tag{6}$$

with a similar relation for the vapour phase. h_j^{L} is the heat transfer coefficient in the liquid phase.

At the vapour–liquid interface we assume phase equilibrium

$$y_{i,j}^{\mathrm{I}} - K_{i,j} x_{i,j}^{\mathrm{I}} = 0 \tag{7}$$

where the superscript I denotes the equilibrium compositions and $K_{i,j}$ the vapour–liquid equilibrium ratio for component i on stage j.

In addition to Eqs. (1)–(7), we have the summation equations for the mole fractions in the vapour and liquid phase and equations expressing the continuity of fluxes of mass and energy across the interface. Furthermore, in the NEQ model we take account of the pressure drop across a stage

$$p_j - p_{j-1} - (\Delta p_{j-1}) = 0 \tag{8}$$

where p_j and p_{j-1} are the stage pressures and Δp_{j-1} the pressure drop per tray from stage $(j-1)$ to stage j. The pressure drop over the stage is considered to be a function of the stage flows, the physical properties and the hardware design.

In the NEQ model, hardware design information must be specified so that mass transfer coefficients, interfacial areas, liquid hold-ups can be calculated. The NEQ model requires thermodynamic properties, not only for calculation of phase equilibrium but also for calculation of driving forces for mass transfer and, in RD, for taking into account the effect of nonideal component behaviour in the calculation of reaction rates and chemical equilibrium constants. In addition, physical properties such as surface tension, diffusion coefficients, viscosities, etc. for calculation of mass (and heat) transfer coefficients and interfacial areas are required. For the most part the property models are those recommended by Reid et al. [18] and by Danner and Daubert [19]. The details of the models used for estimation of diffusivities and mass transfer coefficients are discussed in standard texts [17,20]. The tray design procedure is discussed in detail in [21]. Interested readers can download the technical manual from the ChemSep website: http://www.clarkson.edu/~chengweb/faculty/taylor/chemsep/chemsep.html, which contains details of all thermodynamics, hydrodynamics and mass transfer models for tray and packed columns which have already been implemented into our RD software. The code for these models represents a large fraction of the overall programme size.

For each reaction, we need to know the stoichiometric coefficients, reaction orders, and kinetic constants and whether the reaction is heterogeneous or homogeneous. A homogeneous reaction can also take place in the mass transfer film, the modelling of which requires additional equations for taking into account the effect of the reaction on the interphase mass transfer rate. Finally, we need to know the reaction volume. In the NEQ model, the reaction volume is equal to the total liquid hold-up on a stage; this is obtained directly from the packing specifications and hydrodynamic correlations. For a heterogeneous reaction, there are two options for the description of the reaction term. The simplest way is to treat the reaction pseudo-homogeneously, whereby catalyst diffusion and reaction is lumped into an overall reaction term. In this case, one only needs to specify catalyst weight and activity. This approach is adopted here. A more rigorous approach would involve a more detailed description of diffusion and reaction inside the catalyst particles (see, e.g. [13]). In this case one also needs information about the catalyst geometry (surface area, mean pore diameter, etc).

The steady-state model equations are solved using Newton's method as outlined in [21]. In addition, we have equipped the program with a continuation method for analysis of multiple steady-state behaviour. For more details about this method, the reader is referred to Kubicek [22] and Wayburn and Seader [23].

A further aspect that needs to be considered concerns the modelling of the residence time distribution of the vapour and liquid phases on any "stage". If the column with random dumped or structured packings, it is reasonable to assume that the vapour and liquid phases at any horizontal slice is in true *counter-current* (plug) flow. The situation with respect to vapour–liquid contacting on trays is significantly different. The contacting pattern on any tray, i.e. stage, is *cross-flow* of the vapour and liquid phases. Depending on the flow regime (froth or spray), dispersion height and liquid flow path length each phase (vapour or liquid) could be considered to be in plug flow, well mixed or have a mixing characteristics in between these extremes. Since the residence times and residence time distributions of the liquid and vapour phase can severely affect the performance of a reactor, it is important to develop a proper model to handle these extremes. For this purpose we have adopted the multiple-cells-per-stage approach. In this more recent development each stage is considered to be made up of multiple cells in either fluid phase [11,14]. The vapour–liquid dispersion on a tray is split up in several cells within which interphase mass transfer and subsequent chemical reactions occur. For each of these cells we can write a set of equations as presented above for a single stage. Various forms of mixing behaviour can now be modelled by specifying a number of cells in the direction of flow of the vapour and liquid phases. By varying the number of cells in a flow path we can go from a perfectly mixed phase on a stage (1 cell per flow path), to an approximation of plug flow (large number of cells, typically more than four). In practice the vapour jet issuing from the holes on a tray will create a "fountain" effect; this will tend to mix the liquid phase more or less completely in the vertical direction [20]. In all the calculations presented in this paper involving tray internals, the liquid phase in a vertical column of cells is assumed to be well mixed.

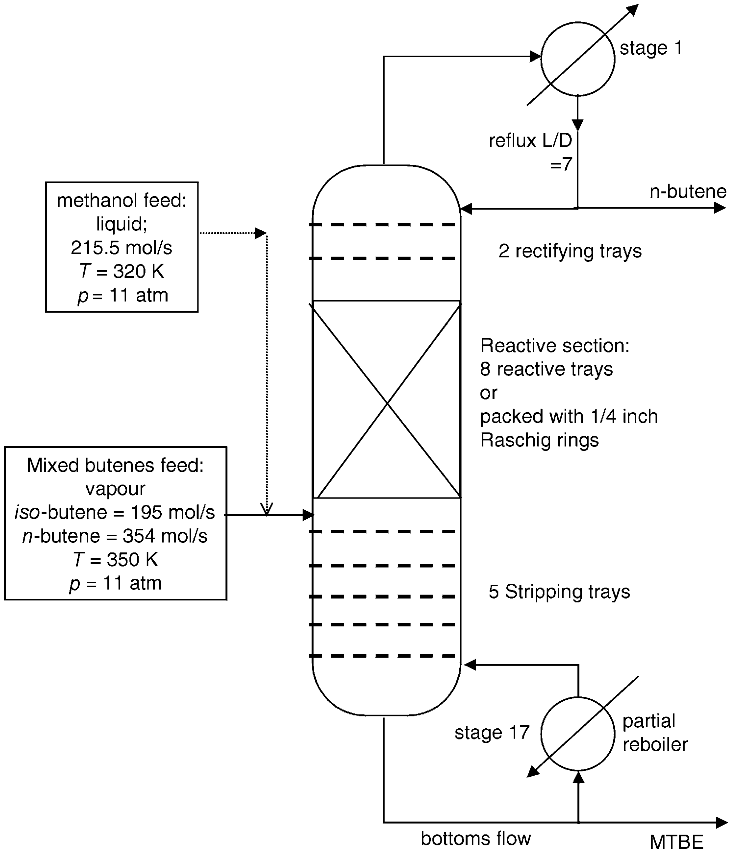

Fig. 2. MTBE column configuration.

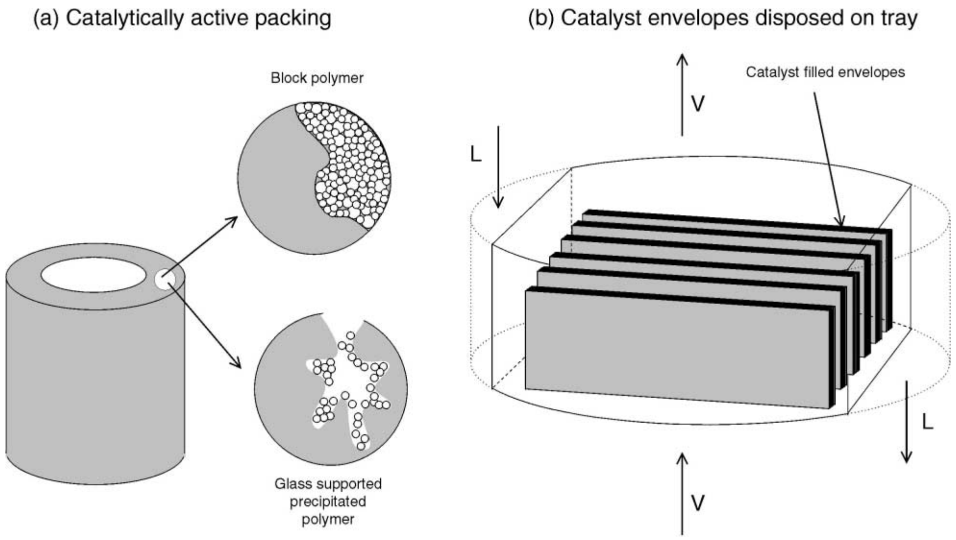

Fig. 3. Catalyst configurations in: (a) packed column; (b) tray column.

3. Simulation study and results

The MTBE synthesis column configuration chosen was essentially that of [24] and shown in Fig. 2. The column diameter was chosen to be 6 m. The stripping and rectifying sections consist of sieve trays. The configuration of the sieve trays are: total tray area $= 28.27\,\mathrm{m}^2$; number of liquid flow passes = 5; tray spacing = 0.7 m; liquid flow path length = 0.97 m; fractional active area = 0.76; fractional hole area = 0.1; fractional downcomer area = 0.12; hole diameter = 4.5 mm; weir height = 50 mm; total weir length = 22 m; weir type = segmental; downcomer clearance = 0.0381 m; tray deck thickness = 25 mm. Two types of configurations have been chosen for the reactive section. Firstly we choose $\frac{1}{4}$ in. random packed Raschig ring shaped catalysts used by Sundmacher and Hoffmann [25] and shown in Fig. 3a. The second choice is that of sieve trays with catalyst envelopes maintained on the trays (see Fig. 3b). Details of this second configuration are available in [26]. The catalyst inventory in the reactive zone is 8000 kg for both hardware configurations. In the base case tray configuration we have chosen the 5-liquid flow pass configuration (see Fig. 4). We also study the influence of the choice of the number of liquid flow passes on the conversion level.

Fig. 5a shows the bifurcation diagram for the packed and tray column configurations for the base case operating conditions. For the reactive tray configuration we

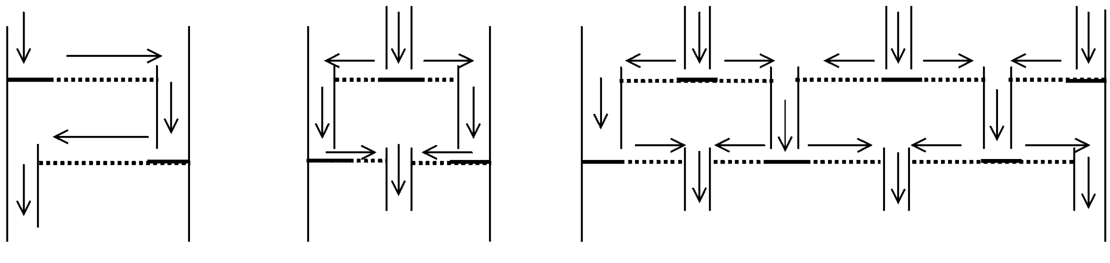

Fig. 4. Tray configurations.

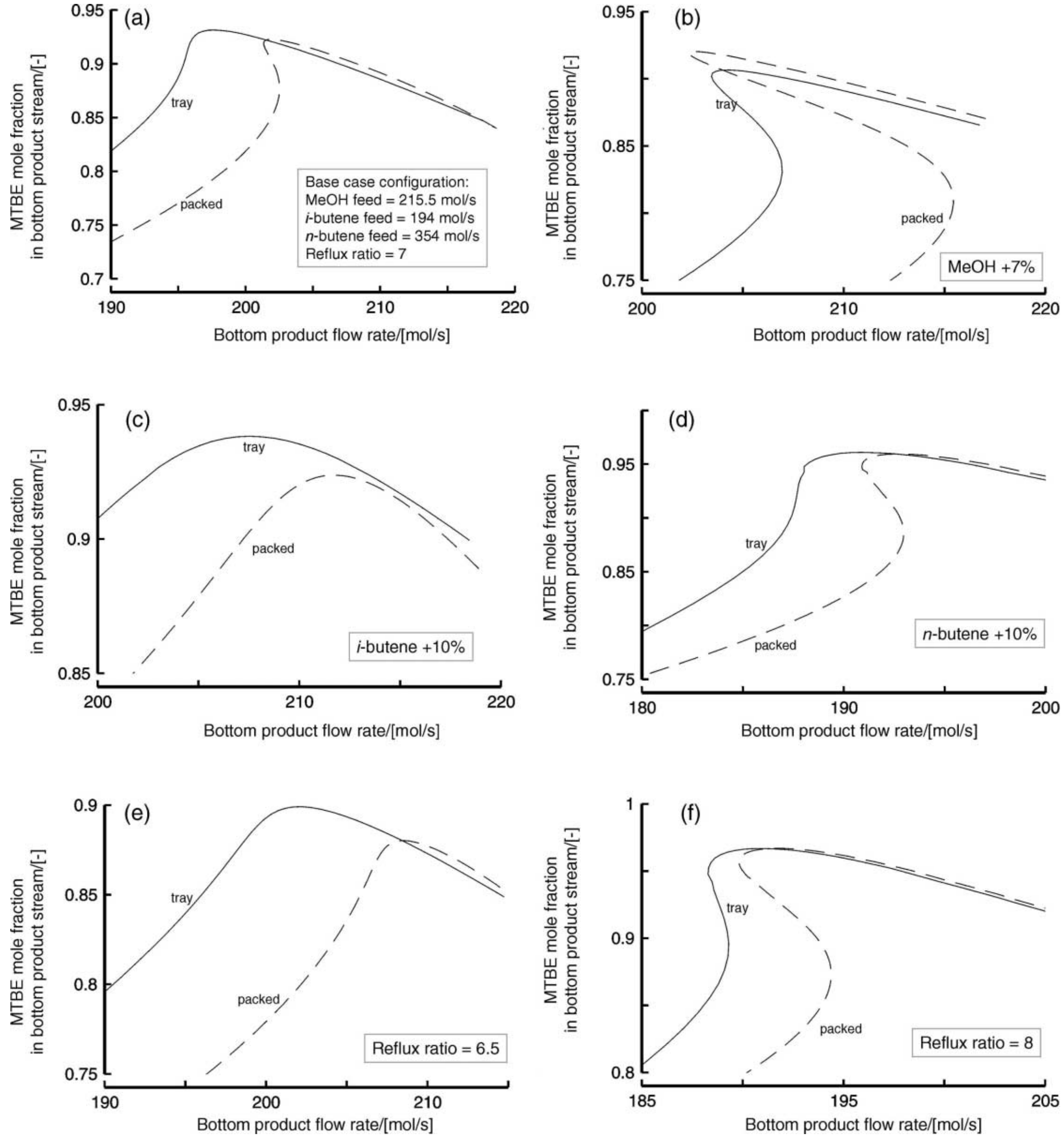

Fig. 5. Bifurcation diagrams for tray and packed columns for various operating conditions.

assumed that both the liquid and vapour phases on the trays are well mixed. If the bottom flow rate were to be set at 202 mol s^{-1}, say, we see that both the packed column shows steady-state multiplicity whereas there is only one steady state for the tray column. For maximising the conversion one must try to operate in the high conversion "branch" of the bifurcation diagram. For this case there is a small conversion advantage for the packed column configuration with respect to the tray configuration. The same trend holds when the MeOH feed is increased by 7%; (see Fig. 5b). We now note that at a bottoms flow of 205 mol s^{-1}, say, both the tray and packed column configurations show steady-state multiplicity. There is a wider range of bottom flows where the tray configuration yields a lower conversion level than the packed column configuration. Fig. 5c

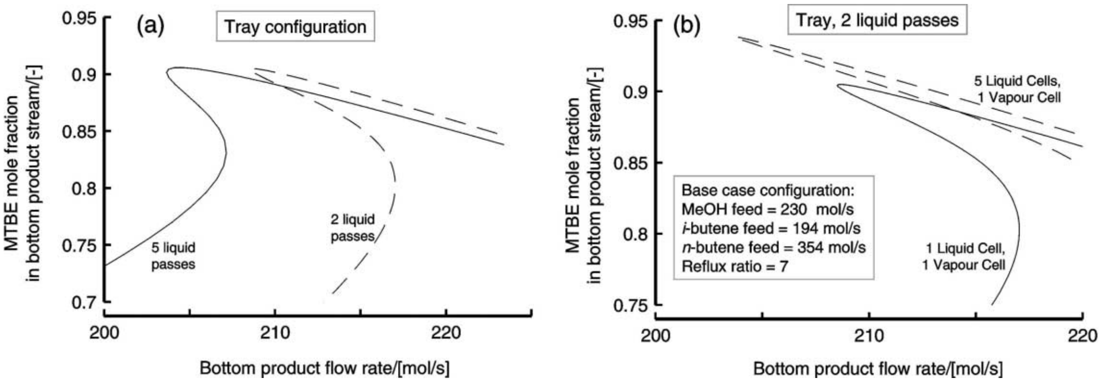

Fig. 6. Bifurcation diagrams for tray column: (a) influence of liquid flow passes; (b) influence of staging of the liquid phase. The operating conditions for both (a) and (b) are specified in the inset to Fig. 6b.

shows the bifurcation diagram for the case in which the iso-butene feed to the column is increased by 10%. No steady-state multiplicity is observed for the tray configurations for either the tray or packed column configurations. The tray configuration is superior to the packed column configuration over the whole range of bottoms flow rates. Fig. 5d shows the bifurcation diagram for the case in which the *n*-butene feed to the column is increased by 10%. No steady-state multiplicity is observed for the tray configuration, whereas the packed column does exhibit steady-state multiplicity. When comparing Fig. 5d with Fig. 5a it is interesting to note that both the tray and packed columns show a slight improvement in the conversion. The reason is that the inerts tend to facilitate the separation of the lighter reactants (MeOH and iso-butene) from the product (MTBE). When the reflux ratio is decreased from 7 to 6.5 (see Fig. 5e), we see that the multiplicity vanishes for both tray and packings. Increasing the reflux ratio to 8, on the other hand (see Fig. 5f), introduces multiplicity for both tray and packed configurations. This means increasing the reflux ratio makes the system more susceptible to disturbances in the operating conditions.

In the calculations shown in Fig. 5, we have assumed 5-liquid flow passes in the reactive section. Fig. 6a shows the effect of reducing the number of liquid flow passes from 5 to 2.

When operating at the high conversion branch, the conversion level increases. Decreasing the number of liquid flow passes increases the liquid load per weir length. This in turn has the effect of increasing the clear liquid height on the tray and the total interfacial area is also increased. A further influence of reducing the number of liquid flow passes is that the vapour and liquid residence times are increased. All of the foregoing serves to improve the conversion, provided one strives to remain on the “high conversion branch”. It is interesting to note that for a column of 6 m diameter, chosen in this study, the conventional wisdom for distillation tray design would be to use multiple flow passes. This does not hold for RD in which we carry out a liquid phase chemical reaction.

In all the foregoing calculations each tray was considered to be one well-mixed stage. We have investigated the influence of introducing staging in the liquid phase. Fig. 6b shows calculations for the 2-liquid pass tray configuration in which the each liquid flow path is considered to be made up of five well-mixed cells. This will ensure near plug flow of the liquid phase. As might be expected the conversion level is significantly improved.

4. Concluding remarks

The tray and packed column configurations show different bifurcation behaviours. When operating on the high conversion branch, the conversions obtained with the tray and packed column configurations are virtually the same. However, performance obtained in the tray column configuration can be improved by decreasing the number of liquid flow passes and thereby increasing the liquid load per weir height and the liquid phase residence time. This results in improved conversion. The NEQ cell model implementation was used to show that if the liquid flow across the tray can be considered to be in plug flow, then this results in a significant improvement in the conversion level. The NEQ model described in this work can be used for hardware choice and optimisation. In a companion paper [14] we show that the hardware choice has a significant effect on the column dynamics.

Acknowledgements

Partial support for our work comes from BP-Amoco Chemicals. RB and RK acknowledge financial support from the Netherlands Organisation for Scientific Research (NWO) in the form of a "programmasubsidie".

References

[1] R. Taylor, R. Krishna, Chem. Eng. Sci. 55 (2000) 5183.
[2] C. Van Gulijk, Comput. Chem. Eng. 22 (1998) S767.
[3] J. Ellenberger, R. Krishna, Chem. Eng. Sci. 54 (1999) 1339.
[4] A.P. Higler, R. Krishna, J. Ellenberger, R. Taylor, Chem. Eng. Sci. 54 (1999) 5145.
[5] R. Krishna, J.M. Van Baten, J. Ellenberger, A.P. Higler, R. Taylor, Chem. Eng. Res. Des. Trans. I. Chem. E 77 (1999) 639.
[6] J.M. Van Baten, R. Krishna, Chem. Eng. J. 77 (2000) 143.
[7] A.P. Higler, R. Taylor, R. Krishna, Comput. Chem. Eng. 22 (1998) S111.
[8] A.P. Higler, R. Taylor, R. Krishna, Chem. Eng. Sci. 54 (1999) 1389.
[9] A.P. Higler, R. Taylor, R. Krishna, Chem. Eng. Sci. 54 (1999) 2873.
[10] A.P. Higler, R. Krishna, R. Taylor, Ind. Eng. Chem. Res. 38 (1999) 3988.
[11] A.P. Higler, R. Krishna, R. Taylor, AIChE J. 45 (1999) 2357.
[12] R. Baur, A.P. Higler, R. Taylor, R. Krishna, Chem. Eng. J. 76 (2000) 33.
[13] A.P. Higler, R. Krishna, R. Taylor, Ind. Eng. Chem. Res. 39 (2000) 1596.
[14] R. Baur, R. Taylor, R. Krishna, Chem. Eng. Sci. 55 (2000) 6139.
[15] R. Taylor, R. Krishna, Multicomponent Mass Transfer, Wiley, New York, 1993.
[16] R. Krishna, J.A. Wesselingh, Chem. Eng. Sci. 52 (1997) 861.
[17] J.A. Wesselingh, R. Krishna, Mass Transfer in Multicomponent Mixtures, Delft University Press, Delft, 2000.
[18] R.C. Reid, J.M. Prausnitz, B.M. Poling, The Properties of Gases and Liquids, 4th Edition, McGraw-Hill, New York, 1988.
[19] R.P. Danner, T.E. Daubert, Manual for Predicting Chemical Process Design Data, AIChE, New York, 1983.
[20] M.J. Lockett, Distillation Tray Fundamentals, Cambridge University Press, Cambridge, 1986.
[21] R. Taylor, H.A. Kooijman, J.S. Hung, Comput. Chem. Eng. 18 (1994) 205.
[22] M. Kubicek, ACM Trans. Math. Software 2 (1976) 98.
[23] T.L. Wayburn, J.D. Seader, Comput. Chem. Eng. 11 (1987) 7.
[24] R. Jacobs, R. Krishna, Ind. Eng. Chem. Res. 32 (1993) 1706.
[25] K. Sundmacher, U. Hoffmann, Chem. Eng. Sci. 49 (1994) 4443.
[26] E.M. Jones Jr., US Patent 4 536 373 (1985).